
Article:
Gibson, J.F., Prajsnar, T.K., Hill, C.J. et al. (8 more authors) (2021) Neutrophils use selective autophagy receptor Sqstm1/p62 to target Staphylococcus aureus for degradation in vivo in zebrafish. Autophagy, 17 (6). pp. 1448-1457. ISSN 1554-8627

https://doi.org/10.1080/15548627.2020.1765521

Neutrophils use selective autophagy receptor Sqstm1/p62 to target *Staphylococcus aureus* for degradation *in vivo* in zebrafish

Josie F Gibson[1,2,3,4,5], Tomasz K Prajsnar[1,2,6], Christopher J Hill[5], Amy K Tooke[5], Justyna J Serba[1,2], Rebecca D Tonge[7], Simon J Foster[4,5], Andrew J Grierson[2,7], Philip W Ingham[3,8#], Stephen A Renshaw[1,2,4#], Simon A Johnston[1,2,4#*].

1. Department of Infection, Immunity and Cardiovascular disease, Medical School, University of Sheffield, S10 2RX UK.
2. The Bateson Centre, University of Sheffield, Sheffield, S10 2TN, UK
3. Institute of Molecular and Cell Biology, Agency of Science, Technology and Research (A-Star), Singapore 138673
4. Florey Institute, University of Sheffield, Sheffield, United Kingdom, S10 2TN
5. Department of Molecular Biology and Biotechnology, University of Sheffield, S10 2TN, UK
6. Institute Biology Leiden, Leiden University, Leiden, The Netherlands
7. Sheffield institute for Translational Neuroscience, Department of Neuroscience, University of Sheffield, S10 2HQ, UK
8. Lee Kong Chian School of Medicine, Nanyang Technological University, Singapore 636921

*Correspondence: s.a.johnston@sheffield.ac.uk
#Joint senior author

Keywords: autophagy, bacterial infection, host-pathogen interactions, neutrophil, *staphylococcus aureus*, SQSTM1/p62, xenophagy, zebrafish.

Abstract

Macroautophagy/autophagy functions to degrade cellular components and intracellular pathogens. Autophagy receptors, including SQSTM1/p62, target intracellular pathogens. *Staphylococcus aureus* is a significant pathogen of humans, especially in immunocompromise. *S. aureus* may use neutrophils as a proliferative niche, but their intracellular fate following phagocytosis has not been analyzed *in vivo*. *In vitro*, SQSTM1 can colocalize with intracellular *Staphylococcus aureus,* but whether SQSTM1 is beneficial or detrimental in host defense against *S. aureus in vivo* is unknown. Here we determine the fate and location of *S. aureus* within neutrophils throughout zebrafish infection. We show Lc3 and Sqstm1 recruitment to phagocytosed *S. aureus* is altered depending on the bacterial location within the neutrophil and that Lc3 marking of bacterial phagosomes within neutrophils may precede bacterial degradation. Finally, we show Sqstm1 is important for controlling cytosolic bacteria, demonstrating for the first time a key role of Sqstm1 in autophagic control of *S. aureus* in neutrophils.

Abbreviations: AR: autophagy receptor; CFU: colony-forming unit; CHT: caudal hematopoietic tissue; GFP: green fluorescent protein; hpf: hours post-fertilization; hpi: hours post-infection; LWT: london wild-type: lyz: lysozyme; Map1lc3/Lc3: microtubule-associated protein 1 light chain 3; RFP: red fluorescent protein; Sqstm1/p62: sequestosome 1; Tg: transgenic; TSA: tyramide signal amplification; UBD: ubiquitin binding domain.

Introduction

Autophagy (macroautophagy) is a process of cellular self-degradation, in which damaged or redundant cellular components are taken into an autophagosome and subsequently trafficked to the lysosome for degradation; these degraded components can then be recycled for alternative uses by the cell [1,2]. During infection, autophagy is used by host cells to degrade invading pathogens, a process termed xenophagy [3,4].

Autophagy is considered largely non-selective of the cargo to be degraded, classically being induced by starvation conditions. However, selective autophagy is a process that enables specific cargo to be directed into the autophagy pathway, which can be used to target invading pathogens. Selective autophagy uses autophagy receptors (ARs), proteins that interact with both autophagy machinery and the cargo to be degraded [5,6]. Many ARs are involved in targeting invading pathogens, including SQSTM1/p62 (sequestosome 1), NBR1 (NBR1 autophagy cargo receptor), OPTN (optineurin) and CALCOCO2/NDP52 (calcium binding and coiled-coil domain 2) [7].

Loss of autophagy function, for example, through mutations in key autophagy genes, can increase the risk of infection with intracellular pathogens [8]. It is well established that pathogen presence can induce host cell autophagy and that pathogens can be degraded by this pathway. Intracellular pathogens such as *Mycobacterium marinum*, *Shigella flexneri* and *Listeria monocytogenes* [9,10] can be targeted by ARs for degradation. Conversely, pathogens have evolved to be able to block or subvert immune defenses, and autophagy is no exception. Indeed, many bacterial pathogens are able to inhibit the induction of autophagy or to reside within the autophagy pathway by preventing lysosomal fusion, or even avoid making any contact with autophagic machinery [11]. In some cases, it is beneficial to the pathogen to up-regulate the autophagy pathway, for example, *Legionella pneumophila, Coxiella burnetii* and *Salmonella enterica* serovar typhimurium [12–14]. The outcome of host-cell autophagy, therefore, differs between various invading pathogens.

Staphylococcus aureus is a bacterial pathogen that can reside within neutrophils as an intracellular niche [15,16]. Autophagy has been implicated in *S. aureus* infection, but there are conflicting reports suggesting autophagy might be either beneficial [17] or detrimental for *S. aureus* [18]. Intracellular pathogens, including *S. aureus*, can escape the phagosome into the cytosol [19], likely through toxins secreted by the bacteria or membrane rupture due to bacterial growth. Once in the cytosol, bacteria can be ubiquitinated and targeted by ARs [7]. Indeed, Sqstm1 in fibroblasts and epithelial cells has been shown to localize to cytosolic *S.*

aureus leading to autophagosome formation *in vitro* [18,20]. Therefore, we investigated whether Sqstm1 recruitment is employed by neutrophils in *S. aureus* infection and what influence selective autophagy has on infection outcome *in vivo*.

In order to examine the role of neutrophil autophagy in *S. aureus* infection, we compared the fate of bacterial cells following Map1lc3/Lc3 (microtubule-associated protein 1 light chain 3) and Sqstm1 recruitment. We tested the role of Sqstm1 in pathogen handling *in vivo*, using the genetic tractability of the zebrafish to create a neutrophil-specific Sqstm1-GFP transgenic reporter and an *sqstm1* activity-deficient mutant. With this approach, we show that Sqstm1 is recruited to cytosolic *S. aureus* and disruption of Sqstm1 expression or function adversely affects *S. aureus* infection outcome.

Results

Staphylococcus aureus *location within neutrophils changes throughout infection.*

Autophagy responses have been demonstrated to change throughout the progression of the infection. Targeting of pathogens by autophagy receptors is likely to occur at later time points in infection. Therefore, to determine the fate and location of *S. aureus* in neutrophils during infection, *S. aureus* expressing mCherry was inoculated and imaged at early (2 to 5 h post-infection [hpi]) and late (24 to 28 hpi) time points. Initially, the well-established *Tg(mpx:eGFP)i114* line that specifically marks neutrophils with EGFP [21] was used to analyze the fate of intracellular *S. aureus* throughout infection. Imaging throughout whole organisms demonstrated a marked reduction in the number of bacterial cells within individual neutrophils, and that the number of neutrophils containing *S. aureus,* between 2 and 24 h post-infection (**Fig. 1A and 1B**). This result suggested to us that neutrophils could degrade intracellular *S. aureus* effectively throughout infection. Indeed, video timelapse of *Tg(mpx:eGFP)i114* larvae infected with mCherry *S. aureus* demonstrated that bacteria could be effectively degraded by the host neutrophils (**Fig. 1C**), although in other cases the bacterial infection is not controlled (**Fig. S1A**).

We next sought to determine the location of bacteria and their association with the autophagic machinery within neutrophils. To do this, we used fluorescently tagged Lc3, as has been demonstrated previously in zebrafish and other models [22–24]. We used a newly generated *Tg(lyz:RFP-GFP-lc3)sh383* [24], a double fusion of RFP and GFP, both linked to Lc3, allowing visualization of Lc3 within neutrophils. We first confirmed that in the caudal hematopoietic tissue (CHT), the infection dynamics were similar to the *Tg(mpx:eGFP)i114* line, with a significant reduction in intracellular bacteria by 26 hpi, indicating bacteria are

efficiently controlled and a significant reduction in infected neutrophils was observed (**Fig. 1D**). Importantly, the number of neutrophils analyzed in the CHT, used for analyses throughout this study, did not significantly change between 2 dpf and 3 dpf (**Fig. S1B**), demonstrating that the change in proportions of infected neutrophils is not due to a large increase in neutrophil number between these time points. The labeling of *S. aureus*-containing vesicles enabled the identification of intracellular bacteria that were within a vesicle (**Fig. 1E**) or free in the cytosol (**Fig. 1F**), as well as non-labeled vesicles, or vesicles marked with Lc3 puncta (**Fig. S1C and S1D**). We found that the proportion of bacteria within vesicles was significantly reduced over time post-injection, whereas the number of bacteria within the cytosol remains relatively constant at a low level, despite becoming proportionally higher relative to vesicular bacteria (**Fig. 1G**). Thus, *S. aureus* phagocytosed by a neutrophil are initially located in a phagocytic vesicle and are subsequently degraded. However, a smaller proportion of *S. aureus* could survive to later infection time points, and these predominantly resided in the cytosol.

Generation and characterisation of an* in vivo *neutrophil GFP-Sqstm1 reporter line.

A previous study identified the co-localization of Sqstm1 with *S. aureus* in non-immune cells [18]. Our findings demonstrated a small but significant population of bacteria that were cytosolic, and therefore a possible target for Sqstm1 binding. Accordingly, we generated a transgenic neutrophil-specific Sqstm1 reporter zebrafish line to examine whether Sqstm1 and intracellular pathogens are co-localized *in vivo*. We used GFP fused via a small linker region to the N-terminus of *sqstm1* in order to produce a fluorescently marked fusion protein expressed within neutrophils via the *lyz* (lysozyme) promoter [25]. Using larvae with double-labeled neutrophils, we were able to identify GFP-expressing cells from the *Tg(lyz:eGFP-sqstm1)i330* reporter line (hereafter called GFP-Sqstm1 reporter) also expressing mCherry (*Tg[lyz:nfsB-mCherry]sh260*) [26] in 98% of neutrophils observed (**Fig. S2A-C**).

We next examined whether the GFP-Sqstm1 protein is able to function as expected. Interestingly, in the double-labeled larvae, GFP puncta but not mCherry puncta were seen (**Fig. S2D**). Similar Sqstm1 puncta that required ubiquitin-binding domain (UBD) to function have been observed *in vitro* for endogenous Sqstm1 [27]. To test whether the GFP-Sqstm1 puncta observed in the GFP-Sqstm1 reporter line respond as expected, GFP-Sqstm1 reporter larvae were treated with autophagy inhibitor Bay K8644: known to block autophagy in zebrafish [29]. As expected, there was a significant increase in the number of neutrophils which contained GFP-Sqstm1 puncta following Bay K8644 treatment in comparison to non-treated controls (**Fig. S2E**), as well as a significant increase in the number of GFP-Sqstm1 puncta within individual neutrophils as expected for endogenous Sqstm1 (**Fig. S2F**). This

result suggests that the GFP-Sqstm1 puncta are not being processed through autophagy and accumulate within the cell, as reported for endogenous Sqstm1 [29]. As we had done for neutrophils and Lc3-positive vesicles, we examined the location of *S. aureus* throughout infection with our GFP-Sqstm1 reporter for consistency with *Tg(mpx:eGFP)i114* and *Tg(lyz:RFP-GFP-lc3)sh383* (**Fig. 1**). We found that there was a comparable reduction in the number of bacteria observed within neutrophils at 26 hpi in comparison to 2 hpi (**Fig. S3A**) and a reduction in the number of infected neutrophils from 2 hpi to 26 hpi (**Fig. S3B**). This result suggested that neutrophils were efficiently degrading these bacteria, in agreement with **Fig. 1**.

Cytosolic bacteria are a possible target for Sqstm1 and *S. aureus* has previously been visualized within the cytosol of a neutrophil from murine infection studies [30].To identify *S. aureus* in the cytosol in our *in vivo* experiments in zebrafish, we looked for regions of the cytosol that co-localized with *S. aureus* but without a reduction of GFP signal, indicating a vacuole excluding the surrounding cytosol (containing GFP). We first confirmed that we could clearly observe phagosomes containing bacteria with low GFP fluorescence consistent with *S. aureus*-containing vacuoles, where host cell cytoplasm containing GFP, was excluded (Sqstm1GFP^{low}, **Fig. S3C**). As further evidence for this analysis, we determined that vesicles containing *S. aureus*, visualized by TEM, were empty of cellular components, in comparison to the cytosol (**Fig. S3D**), suggesting GFP^{low} areas represent vesicles. Finally, we looked for functional differences consistent with the presence of a phagosomal membrane in GFP^{low} regions by examining pH differences using the pH-sensitive dye pHrodo. We found examples of low pH in vesicles correlating with low cytoplasmic fluorescence (**Fig. S3E**), again suggesting GFP^{low} areas represent vesicles. Having characterized features consistent with an *S. aureus*-containing vacuoles, we were able to assign a subset of bacteria as being in either a damaged phagosome or located in the cytosol (Sqstm1GFP^{high}, **Fig. S3F**). For the purpose of this study, we are defining these bacteria as cytosolic, as they are accessible to cytosolic proteins. We then assigned the cellular location of *S. aureus* by these features at 2 hpi and 26 hpi. We determined that the proportion of *S. aureus* within vesicles was significantly reduced by 26 hpi (**Fig. S3G**) and that the number of bacteria within the cytosol is similar at both time points, in agreement with our *Tg(lyz:RFP-GFP-lc3)sh383* data (**Fig. 1**).

Lc3 and Sqstm1 are recruited to* Staphylococcus aureus *within neutrophils.

We determined that GFP-Sqstm1 puncta co-localize with *S. aureus* either marking a vesicle containing *S. aureus* (**Fig. 2A and Video S1**) or directly in contact with *S. aureus* located in the cytosol (**Fig. 2B and Video S2**). For puncta marking *S. aureus* in vesicles, no difference

in the proportion of vesicles marked was observed at 2 or 26 hpi, although the actual number of puncta-marking vesicles was dramatically reduced by 26 hpi (**Fig. 2C**) as most bacteria had already been degraded. GFP-puncta-marking bacteria in the cytosol were decreased at 26 hpi (**Fig. 2D**), as expected, given that Sqstm1 is degraded with the cargo targeted for degradation [29]. We previously showed cytosolic GFP-Sqstm1 puncta were modulated by autophagy machinery-targeting drugs (**Fig. S2E and S2F**). In further agreement with this, comparison between infected and uninfected neutrophils showed there was no difference in the number of cytoplasmic GFP-Sqstm1 puncta at 2 hpi but a significant reduction by 26 hpi (**Fig. 2E and 2F),** indicating these puncta are modulated by *S. aureus* infection.

We next examined whether Lc3 can localize to vesicular and cytosolic *S. aureus*. At 2 hpi and 26 hpi, there was no difference in the proportion of vesicles marked by Lc3, but most vesicular bacteria are degraded by 26 hpi (**Fig. 2G**), showing that a rapid Lc3 response to *S. aureus* infection occurs. In contrast, vesicles containing *S. aureus* are significantly more likely to have Lc3 puncta associated at 2 hpi (**Fig. 2H and S1D**). However, most bacteria are still cleared by 26 hpi, and there was no significant change in the association of Lc3 puncta to *S. aureus* in the cytosol over time (**Fig. 2I**).

Loss of Sqstm1 reduces zebrafish survival following* S. aureus *infection.

We had demonstrated the steps of Lc3 and the autophagy receptor Sqstm1 recruitment *in vivo* in the degradation of *S. aureus* by neutrophils, suggesting a function for Sqstm1 in immunity to *S. aureus* infection by targeting the degradation of bacteria that escaped the phagosome. To test this prediction, we examined the role of Sqstm1 in *S. aureus* zebrafish infection using a morpholino-modified antisense oligonucleotide (morpholino) targeting *sqstm1* [31] to knockdown *sqstm1* expression in the zebrafish larvae. Knockdown of *sqstm1* resulted in a significant reduction in zebrafish survival following *S. aureus* infection, compared to control larvae, supporting a requirement for *sqstm1* in the control of *S. aureus* infection (**Fig. 3A**). Knockdown of *sqstm1* did not reduce larval survival for heat-killed *S. aureus* or the non-virulent but closely related bacterium *Micrococcus luteus* (**Fig. S3I and S3J**), suggesting Sqstm1 is important for restriction of pathogenic bacteria that escape the phagosome. To further support this conclusion, we generated an *sqstm1* mutant zebrafish (sh558) that lacked a functional UBD domain in *sqstm1*, inhibiting the ability of Sqstm1 to bind to ubiquitinated cargo (**Fig. 3C**). In agreement with our knockdown study, the *sqstm1* mutant zebrafish (sh558) larvae were significantly more susceptible to *S. aureus* infection than wild-type control zebrafish (**Fig. 3B**). Thus, in addition to demonstrating how Lc3 and Sqstm1 were localized during intracellular handling of *S. aureus* by neutrophils, we could independently show the requirement of Sqstm1 in the outcome of infection.

Both *sqstm1* morpholino and *sqstm1* mutant zebrafish (sh558) techniques do not block Sqstm1 function in neutrophils specifically; therefore, we next aimed to determine whether the loss of Sqstm1 was important in neutrophils during *S. aureus* infection. Interestingly, there was no difference between the survival of our GFP-Sqstm1 reporter and wild-type controls (**Fig. S3H**), suggesting that endogenous *sqstm1* expression is sufficient for restriction of the small proportion of bacteria which reside in the cytosol. First, using tyramide signal amplification (TSA) staining of 1 dpi larvae to visualize neutrophils within *sqstm1* mutant (sh558) and control larvae, we found a non-significant (p=0.1039) increase in neutrophils containing *S. aureus* (**Fig. 3D**). A small effect was expected due to the small proportion of cytosolic bacteria, which are likely targeted by Sqstm1 during infection. It was, therefore, likely that showing a difference in the number of infected neutrophils would have required a very large number of infections. We were able to calculate that the observed differences would require a group size of 270.

Next, using *sqstm1* morphants and control larvae, a comparison of the number of bacteria present within neutrophils at 1 dpi was completed in the *Tg(mpx:eGFP)i114 larvae*. In agreement with the Sqstm1-UBD mutant data, a non-significant (p=0.115) increase of neutrophils containing *S. aureus* was observed in *sqstm1* morphants in comparison to wild-type controls (**Fig. 3E**). Again, we had calculated that the observed differences would require a large group size of 219. However, the examination of the bacterial location revealed a significant increase in the number of cytosolic *S. aureus* in the *sqstm1* morphants in comparison to control fish (**Fig. 3F**), suggesting loss of Sqstm1 is important for the control of cytosolic *S. aureus* by neutrophils. Thus, we could show that loss of *sqstm1* leads to an increase in bacterial burden within neutrophils and that Sqstm1 is likely targeting the small proportion of bacteria that escape to the cytosol.

Discussion

Using the unique attributes of long-term high-resolution imaging and genetic manipulation of zebrafish larvae, we have shown the dynamics of Lc3 and Sqstm1 on the *S. aureus*-containing vacuoles, their relation to bacterial degradation, and how Sqstm1 recognizes cytosolic bacteria, meaning that loss of Sqstm1 activity is sufficient to increase mortality following *S. aureus* infection.

Loss of zebrafish *sqstm1*, through morpholino-mediated knockdown, significantly increased susceptibility to the infection to *S. aureus*. This result is the first *in vivo* evidence that Sqstm1 is important in the outcome of intracellular handling of *S. aureus*. To confirm the *sqstm1* knockdown data, we generated a zebrafish *sqstm1* mutant lacking the UBD domain, which confirmed a significant increase in the susceptibility of zebrafish to *S. aureus* infection. This result suggests that for *S. aureus* infection control, the Sqstm1 UBD, which can bind to

ubiquitinated *S. aureus* [18,20], is important for host control of infection. In addition to its role as an autophagy receptor, Sqstm1 can aid in the killing of pathogens through the delivery of anti-microbial peptides [32]. Thus, it is possible that anti-microbial peptides delivered by Sqstm1 are important in neutrophil control of *S. aureus* infection. The *sqstm1* zebrafish mutant represents a valuable tool in the analysis of selective autophagy in infection, which may also be useful for the study of other intracellular pathogens or in other diseases, where autophagy is implicated in pathology, for example in neurodegenerative disorders.

Although *in vitro* studies have described co-localization of Sqstm1 and autophagy in pathogen handling, until now, no evidence of direct Sqstm1 interactions with these pathogens has been shown in neutrophils or *in vivo*. Interaction of Sqstm1 with *S. aureus* has been demonstrated through *in vitro* studies using fibroblasts and epithelial cells [18,20]. *In vitro* data shows *S. aureus* can be targeted for autophagic degradation by Sqstm1 [18,20], where puncta appear to be co-localized with *S. aureus*. Our new zebrafish GFP-Sqstm1 reporter shows cytosolic puncta formation, which has also been observed in other cell culture studies, both endogenous expression and using similar GFP-Sqstm1 reporter systems [27,33,34]. By comparing GFP-Sqstm1 puncta marking of intracellular *S. aureus* with the location of bacteria over time, it is interesting to note that Sqstm1 marking is reduced over time for cytosolic bacteria, which appear to be a small population that persists throughout infection. This result may indicate that cytosolic bacteria marked with Sqstm1 are degraded. Furthermore, at later time points in *S. aureus* infection, the number of GFP-Sqstm1 puncta is reduced within infected cells, suggesting that when bacteria escape the phagosome, Sqstm1 becomes important in controlling cytosolic bacteria.

We show that most *S. aureus* is contained within a vesicle soon after infection, and by 26 hpi, most *S. aureus* are absent from neutrophils. Of note, some images show bacteria outside the neutrophils that have been phagocytosed by macrophages, which has previously been described [35]. The large reduction of neutrophils containing bacteria from 2 hpi to 26 hpi, leaving a small population at 26 hpi, may be representative of a niche for bacterial persistence and/or proliferation. The role of neutrophils as an intracellular niche has previously been described to be important in determining the outcome of *S. aureus* infection [15,16,36]. Interestingly, it appears that Lc3 marks the majority of vesicles containing bacteria. Lc3 localization to *S. aureus* may represent Lc3 recruitment to autophagosomes; however, since recruitment is observed at early infection time points, it may represent Lc3-associated phagocytosis, which is also observed in *Listeria monocytogenes* infection of macrophages [37]. Since most bacteria are degraded, it appears that Lc3 marking of vesicles could lead to bacterial degradation in the zebrafish.

Thus, we demonstrate that host Sqstm1 is beneficial for the host outcome following *S. aureus* infection and that Sqstm1-mediated control of cytosolic bacteria within neutrophils

may represent one of many mechanisms employed by the host in immunity to this versatile pathogen.

Materials and methods

Ethics statement.

Animal work was carried out according to guidelines and legislation set out in UK law in the Animals (Scientific Procedures) Act 1986, under Project License PPL 40/3574 or P1A4A7A5E). Ethical approval was granted by the University of Sheffield Local Ethical Review Panel. Animal work completed in Singapore was completed under the Institutional Animal Care and Use Committee (IACUC) guidelines under the A*STAR Biological Resource Centre (BRC) approved IACUC Protocol #140977.

Zebrafish husbandry.

Zebrafish strains were maintained according to standard protocols [38]. For animals housed in the Bateson Centre aquaria at the University of Sheffield, adult fish were maintained on a 14:10-h light/dark cycle at 28°C in UK Home Office approved facilities. For animals housed in IMCB, Singapore, adult fish were maintained on a 14:10-h light/dark cycle at 28°C in the IMCB zebrafish facility. London wild-type (LWT) and AB wild-type larvae were used in addition to transgenic lines, *Tg(lyz:eGFP-sqstm1)i330* created in this study, *Tg(lyz:RFP-GFP-Lc3)sh383* [24], *Tg(lyz:nfsB-mCherry)sh260* [26] (these fish encode nitroreductase gene *nsfB* within neutrophils which allows ablation of cells following metronidazole treatment, which was not used in this study) and *Tg(mpx:eGFP)i114* [21]. Generation of Sqstm1 sh558 mutant zebrafish is described below. Larvae were maintained in E3 (5 mM NaCl, 0.17 mM KCl, 0.33 mM CaCl2, 0.33 mM MgSO4) plus methylene blue (Sigma-Aldrich, 50484) at 28°C until 5 dpf.

S. aureus *culture.*

The *Staphylococcus aureus* strain SH1000 [39] was used in this study. A single bacterial colony was placed in 10 ml brain heart infusion medium (Thermo Fisher Scientific, OxoidCM1135B) overnight at 37°C, 250 rpm. 500 µl of this overnight culture was then added to 50 ml of brain heart infusion medium and incubated at 37°C, 250 rpm until OD_{600} 1. The bacteria were then pelleted at 5445 x g, 4°C for 15 min. The bacteria were then resuspended in PBS (Oxoid, BR0014G), using a volume to dilute to the required dose, with 1500 colony-forming units (cfu)/nL being standard. Bacteria were incubated on ice for a short period, until use. Strains used: SH1000 wild-type strain [39], SH1000-pMV158-mCherry [40], SH1000-pMV158-GFP [40].

Zebrafish micro-injection.

For *sqstm1* morpholino microinjections: Larvae were injected immediately after fertilization using an *sqstm1* morpholino [31]. A standard control morpholino (Genetools) was used as a negative control. For injection of *S. aureus,* zebrafish larvae were injected at 1 dpf (for survival analysis, [36]) or 2 dpf (for microscopy analysis) and monitored until a maximum of 5 dpf. Larvae were anesthetized by immersion in 0.168 mg/mL tricaine (Pharmaq Ltd, ATC QN01AX93) in E3 and transferred onto 3% methyl cellulose (Sigma-Aldrich, M0387) in E3 for injection. For *S. aureus* 1 nl of bacteria, containing 1500 cfu, was injected into the yolk sac circulation valley. Larvae were transferred to fresh E3 to recover from anesthetic. Any zebrafish injured by the needle/micro-injection were removed from the procedure. Zebrafish were maintained at 28°C.

Generation of* Tg(lyz:eGFP-sqstm1)i330 *transgenic line.

The generation of the *Tg(lyz:eGFP-sqstm1)i330* line was performed using the Gateway™ system in combination with Tol2 transgenesis [41]. To make the required expression clone, *pDest(lyz:eGFP-sqstm1)*, the *p5E-lyz* entry clone [42] and the *pME-eGFP-nostop* [41] middle entry vectors were used. The destination vector *pDesttol2CG* [41], was chosen, which included *tol2* sites for integration into the genome, in addition to a GFP heart marker. The required *sqstm1* 3' entry vector and expression clone *pDest(lyz:eGFP-sqstm1)* were constructed following the Multisite Gateway™ three-fragment vector construction kit (Invitrogen, 12537-023). To generate *tol2* mRNA, a pCS2FA-transposase plasmid [41] was used. The DNA plasmid was linearized through a restriction site digest. *tol2* mRNA was generated by a transcription reaction (Ambion T3 mMessage Machine). *tol2* mRNA and *pDest(lyz:eGFP-sqstm1)* were co-injected into a single cell (at the single cell stage) of wild-type AB larvae. A 1 nl injection contained 30 pg of *tol2* mRNA and 60 pg of *pDest(lyz:eGFP-sqstm1)*.

Microscopy of infected zebrafish.

Larvae were anesthetized 0.168 mg/mL tricaine in E3 and mounted in 0.8% low melting agarose (Affymetrix, 32830) onto glass-bottom microwell dishes (MatTek, P35G-1.5-14C). An UltraVIEW VoX spinning disk confocal microscope (Perkin Elmer, Cambridge, UK) was used for imaging neutrophils within larvae. 405-nm, 445-nm, 488-nm, 514-nm, 561-nm and 640-nm lasers were available for excitation. Most cellular level imaging was completed in the

caudal hematopoietic tissue (CHT) using a 40x oil objective (UplanSApo 40x oil [NA 1.3]). In some cases, a 20x objective was used for whole larvae imaging. GFP, TxRed emission filters were used and bright-field images were acquired using a Hamamatsu C9100-50 EM-CCD camera. Volocity software was used. Between early and late time points, zebrafish larvae were placed back into E3 and maintained at 28°C.

pHrodo staining of* S. aureus*.

Bacterial strains were prepared for injected (as above) and resuspended into PBS pH 9. pHrodo (Thermo Fisher Scientific, P36600) was added at a ratio of 1:200 and incubated at 37°C for 30 min, shaking, in the dark. The bacteria were suspended in PBS pH 8 and washed through a series of solutions (Tris, pH 8.5, PBS pH 8) and finally resuspended into PBS pH 7.4 for injection.

Tyramide Signal Amplification (TSA) Staining.

Following *S. aureus* infection, larvae were fixed in paraformaldehyde (Thermo Fisher Scientific, 28908) diluted to 4% in PBS, overnight at 4°C. Once fixed, larvae were washed in PBS thrice. Staining of neutrophils (specifically myeloperoxidase activity) in LWT larvae was completed using TSA staining kit (Cy5-TSA Cyanine Kit; PerkinElmer, NEL705A001KT). Fish were incubated in a 1:100 ratio of Cy5-TSA:amplification diluent at 28°C for 10 min in the dark. Larvae were washed thrice in PBS before imaging.

TEM of infected zebrafish.

Specimens were fixed in 2.5% glutaraldehyde (Agar Scientific, AGR1010), in 0.1 M sodium cacodylate (Agar Scientific, AGR1105) and post-fixed 2% aqueous osmium tetroxide, dehydrated through graded series of ethanol, and cleared in propylene oxide (Agar Scientific, AGR1080) and then infiltrated in 50:50 Araldite resin (Araldite resin made up of a 50:50 dodecenyl succinic anhydride (Agar Scientific, AGR1051) and Araldite resin CY212 (Agar Scientific, AGR1040) mix plus 1 drop/ml benzyl dimethylamine (Agar Scientific, AGR1060) and propylene oxide (Agar Scientific, AGR1080) mixture overnight on a rotor. This mixture was replaced with two changes over 8 h of fresh Araldite resin mixture before being embedded in fresh resin and cured in a 60°C oven for 48-72 h. Ultrathin sections, approximately 85-nm thick, were cut on a Leica UC6 ultramicrotome onto 200-mesh copper grids (Agar Scientific, G2200C). These were stained for 10 min with saturated aqueous uranyl acetate followed by Reynolds lead citrate [43] for 5 min. Sections were examined

using a FEI Tecnai Transmission Electron Microscope at an accelerating voltage of 80 kV. Electron micrographs were recorded using Gatan Orius 1000 digital camera and Gatan Digital Micrograph software.

Image analysis.

Image analysis was performed using ImageJ software [44] to quantify the number of *S. aureus* cells within neutrophils and to quantify GFP-Sqstm1 puncta and Lc3 co-localization to these pathogens.

Drug treatment of zebrafish.

Larvae were treated with an autophagy inhibitor through immersion in E3 medium. Bay K8644 (Sigma-Aldrich, B2112) was added to the E3 to the required concentration of 1 µM. Larvae were incubated at 28°C for 24 h before microscopy. Zebrafish were not anesthetized for immersion drug treatments.

Generation of* sqstm1 *mutant.

A zebrafish *sqstm1* mutant was generated using CRISPR-Cas9 mutagenesis. A guide RNA targeting exon 8 of zebrafish *sqstm1* (ACAGAGACTCCACCAGCCTA) was inserted into a published oligonucleotide scaffold [45] and injected together with recombinant Cas9 protein (New England Biolabs) into 1-2 cell stage zebrafish (AB strain). Efficiency of mutagenesis was confirmed using high-resolution melt curve analysis as previously described [46] and several founders were identified. *sqstm1*^{sh558} carries a 10-base pair deletion resulting in a frameshift and premature truncation of Sqstm1 in the ubiquitin-associated (UBA) domain.

Statistical analysis.

Statistical analysis was performed as described in the results and figure legends. We used Graph Pad Prism 7 (v7.04) for statistical tests and plots. Fisher's exact tests, which are reliable with very small group sizes, were used to analyze data sets that have uneven group sizes. In these cases, small group sizes were unavoidable due to the nature of these experiments in which we describe only a very small proportion of bacterial cells are observed at later time points in zebrafish infection.

Acknowledgments

JFG was supported by an award from the Singapore A*STAR Research Attachment Programme (ARAP) in partnership with the University of Sheffield, and a Medical Research Council Grant (MR/R001111/1 with SAR and SJF). TKP was supported by an individual Marie Curie fellowship (PIEF-GA-2013-625975) and by AMR cross-council funding from the MRC to the SHIELD consortium "Optimising Innate Host Defence to Combat Antimicrobial Resistance" MRNO2995X/1. RDT and AJG were supported by the University of Sheffield. JJS was a Marie Curie fellow in the Initial Training Network FishForPharma (PITN-GA-2011-289209). Work in the PWI lab was funded by the A*STAR Institute of Molecular and Cell Biology (IMCB) and the Lee Kong Chian School of Medicine. SAJ was supported by the Medical Research Council and Department for International Development Career Development Award Fellowship MR/J009156/1 (http://www.mrc.ac.uk/). SAJ was additionally supported by a Krebs Institute Fellowship (http://krebsinstitute.group.shef.ac.uk/), and Medical Research Council Centre grant (G0700091). SAR was supported by a Medical Research Council Programme Grant (MR/M004864/1) (http://www.mrc.ac.uk/). Imaging was completed at the Wolfson Light Microscopy Facility. We thank the aquarium staff at the Bateson Centre (Sheffield) and the IMCB (Singapore) for zebrafish husbandry.

Declaration of interest statement

The authors have no conflict of interests

References

1. Mizushima N, Levine B, Cuervo A, Klionsky D. Autophagy fights disease through cellular self-digestion. Nature. 2008;451(7182):1069–75.
2. Tanida I. Autophagy basics. Microbiol Immunol. 2011 Jan;55(1):1–11.
3. Gatica D, Lahiri V, Klionsky DJ. Cargo recognition and degradation by selective autophagy. Nat Cell Biol. 2018 Mar;20(3):233–42.
4. Sharma V, Verma S, Seranova E, Sarkar S, Kumar D. Selective Autophagy and Xenophagy in Infection and Disease. Front cell Dev Biol. 2018;6:147.
5. Popovic D, Dikic I. The molecular basis of selective autophagy. Biochem (Lond). 2012;34(2):24–30.
6. Rogov V, Dötsch V, Johansen T, Kirkin V. Interactions between autophagy receptors and ubiquitin-like proteins form the molecular basis for selective autophagy. Mol Cell. 2014 Jan;53(2):167–78.
7. Farré J-C, Subramani S. Mechanistic insights into selective autophagy pathways: lessons from yeast. Nat Rev Mol Cell Biol. 2016 Jul 6;17(9):537–52.
8. Levine B, Mizushima N, Virgin H. Autophagy in immunity and inflammation. Nature. 2011;469(7330):323–35.
9. Zhang R, Varela M, Vallentgoed W, Forn-Cuni G, van der Vaart M, Meijer AH. The selective autophagy receptors Optineurin and p62 are both required for zebrafish host resistance to mycobacterial infection. Behr MA, editor. PLOS Pathog. 2019 Feb 28;15(2):e1007329.
10. Mostowy S, Sancho-Shimizu V, Hamon MA, Simeone R, Brosch R, Johansen T, et al. p62 and NDP52 proteins target intracytosolic Shigella and Listeria to different autophagy pathways. J Biol Chem. 2011 Jul 29;286(30):26987–95.
11. Deretic V, Levine B. Autophagy, immunity, and microbial adaptations. Cell Host Microbe. 2009;5(6):527–49.
12. Amer AO, Swanson MS. Autophagy is an immediate macrophage response to Legionella pneumophila. Cell Microbiol. 2005 Jun;7(6):765–78.
13. Hernandez LD, Pypaert M, Flavell R a, Galán JE. A Salmonella protein causes macrophage cell death by inducing autophagy. J Cell Biol. 2003 Dec 8;163(5):1123–31.
14. Gutierrez MG, Vázquez CL, Munafó DB, Zoppino FCM, Berón W, Rabinovitch M, et al. Autophagy induction favours the generation and maturation of the Coxiella-replicative vacuoles. Cell Microbiol. 2005 May 12;7(7):981–93.
15. Thwaites GE, Gant V. Are bloodstream leukocytes Trojan Horses for the metastasis of Staphylococcus aureus? Nat Rev Microbiol. 2011 Mar 7;9(3):215–22.
16. Prajsnar TK, Hamilton R, Garcia-Lara J, McVicker G, Williams A, Boots M, et al. A privileged intraphagocyte niche is responsible for disseminated infection of Staphylococcus aureus in a zebrafish model. Cell Microbiol. 2012 Oct;14(10):1600–19.
17. Schnaith A, Kashkar H, Leggio SA, Addicks K, Krönke M, Krut O. Staphylococcus aureus subvert autophagy for induction of caspase-independent host cell death. J Biol Chem. 2007 Jan 26;282(4):2695–706.
18. Neumann Y, Bruns SA, Rohde M, Prajsnar TK, Foster SJ, Schmitz I. Intracellular *Staphylococcus aureus* eludes selective autophagy by activating a host cell kinase. Autophagy. 2016 Nov 14;12(11):2069–84.
19. Bayles KW, Wesson CA, Liou LE, Fox LK, Bohach GA, Trumble WR. Intracellular Staphylococcus aureus escapes the endosome and induces apoptosis in epithelial cells. Infect Immun. 1998 Jan;66(1):336–42.
20. Singh A, Patel P, Tomar D, Singh R, Sripada L, Prajapati P, et al. TBK1 regulates p62/sqstm1 mediated autophagic clearance of intracellular ubiquitinated Staphylococcus aureus in human epithelial cells. Transl Genet genomics. 2017;[online fi.
21. Renshaw SA, Loynes CA, Trushell DMI, Elworthy S, Ingham PW, Whyte MKB. A transgenic zebrafish model of neutrophilic inflammation. Blood. 2006;108(13).

22. Mathai B, Meijer A, Simonsen A. Studying Autophagy in Zebrafish. Cells. 2017 Jul 9;6(3):21.
23. Li L, Wang Z V., Hill JA, Lin F. New Autophagy Reporter Mice Reveal Dynamics of Proximal Tubular Autophagy. J Am Soc Nephrol. 2014 Feb;25(2):305–15.
24. Prajsnar TK, Serba JJ, Dekker BM, Gibson JF, Masud S, Fleming A, et al. The autophagic response to Staphylococcus aureus provides an intracellular niche in neutrophils. bioRxiv. 2019 Mar 18;581223.
25. Yang C-T, Cambier CJ, Davis JM, Hall CJ, Crosier PS, Ramakrishnan L. Neutrophils exert protection in the early tuberculous granuloma by oxidative killing of mycobacteria phagocytosed from infected macrophages. Cell Host Microbe. 2012 Sep 13;12(3):301–12.
26. Buchan KD, Prajsnar TK, Ogryzko N V, Jong NW de, Gent M van, Kolata J, et al. A transgenic zebrafish line for in vivo visualisation of neutrophil myeloperoxidase. bioRxiv. 2019 Mar 20;456541.
27. Bjørkøy G, Lamark T, Brech A, Outzen H, Perander M, Øvervatn A, et al. p62/SQSTM1 forms protein aggregates degraded by autophagy and has a protective effect on huntingtin-induced cell death. J Cell Biol. 2005;171(4).
28. Williams A, Sarkar S, Cuddon P, Ttofi EK, Saiki S, Siddiqi FH, et al. Novel targets for Huntington's disease in an mTOR-independent autophagy pathway. Nat Chem Biol. 2008 May;4(5):295–305.
29. Bjørkøy G, Lamark T, Pankiv S, Øvervatn A, Brech A, Johansen T. Chapter 12 Monitoring Autophagic Degradation of p62/SQSTM1. In 2009. p. 181–97.
30. Gresham HD, Lowrance JH, Caver TE, Wilson BS, Cheung AL, Lindberg FP. Survival of Staphylococcus aureus inside neutrophils contributes to infection. J Immunol. 2000 Apr 1;164(7):3713–22.
31. van der Vaart M, Korbee CJ, Lamers GEM, Tengeler AC, Hosseini R, Haks MC, et al. The DNA Damage-Regulated Autophagy Modulator DRAM1 Links Mycobacterial Recognition via TLR-MYD88 to Autophagic Defense. Cell Host Microbe. 2014 Jun 11;15(6):753–67.
32. Ponpuak M, Davis AS, Roberts EA, Delgado MA, Dinkins C, Zhao Z, et al. Delivery of cytosolic components by autophagic adaptor protein p62 endows autophagosomes with unique antimicrobial properties. Immunity. 2010 Mar 26;32(3):329–41.
33. Larsen KB, Lamark T, øvervatn A, Harneshaug I, Johansen T, Bjørkøy G. A reporter cell system to monitor autophagy based on p62/SQSTM1. Autophagy. 2010;66:784–93.
34. Pankiv S, Clausen TH, Lamark T, Brech A, Bruun J-A, Outzen H, et al. p62/SQSTM1 binds directly to Atg8/LC3 to facilitate degradation of ubiquitinated protein aggregates by autophagy. J Biol Chem. 2007 Aug 17;282(33):24131–45.
35. Prajsnar TK, Cunliffe VT, Foster SJ, Renshaw S a. A novel vertebrate model of Staphylococcus aureus infection reveals phagocyte-dependent resistance of zebrafish to non-host specialized pathogens. Cell Microbiol. 2008 Nov;10(11):2312–25.
36. Pollitt EJG, Szkuta PT, Burns N, Foster SJ. Staphylococcus aureus infection dynamics. PLoS Pathog. 2018;14(6):e1007112.
37. Gluschko A, Herb M, Wiegmann K, Krut O, Neiss WF, Utermöhlen O, et al. The β2 Integrin Mac-1 Induces Protective LC3-Associated Phagocytosis of Listeria monocytogenes. Cell Host Microbe. 2018 Mar 14;23(3):324-337.e5.
38. Nüsslein-Volhard C (Christiane), Dahm R. Zebrafish : a practical approach. Oxford University Press; 2002.
39. Horsburgh MJ, Aish JL, White IJ, Shaw L, Lithgow JK, Foster SJ, et al. Omega B Modulates Virulence Determinant Expression and Stress Resistance: Characterization of a Functional rsbU Strain Derived from Staphylococcus aureus 8325-4. J Bacteriol. 2002;184(19):5457–67.
40. Boldock E, Surewaard BGJ, Shamarina D, Renshaw S, Foster S. Human skin commensals augment Staphylococcus aureus pathogenesis. Nat Microbiol. 2018;3:881–90.

631 41. Kwan KM, Fujimoto E, Grabher C, Mangum BD, Hardy ME, Campbell DS, et al. The
632 Tol2kit: A multisite gateway-based construction kit forTol2 transposon transgenesis
633 constructs. Dev Dyn. 2007 Nov;236(11):3088–99.
634 42. Elks PM, van Eeden FJ, Dixon G, Wang X, Reyes-Aldasoro CC, Ingham PW, et al.
635 Activation of hypoxia-inducible factor-1α (Hif-1α) delays inflammation resolution by
636 reducing neutrophil apoptosis and reverse migration in a zebrafish inflammation
637 model. Blood. 2011 Jul 21;118(3):712–22.
638 43. Reynolds ES. The use of lead citrate at high pH as an electron-opaque stain in
639 electron microscopy. J Cell Biol. 1963 Apr;17(1):208–12.
640 44. Rasband WS. ImageJ. U.S. National Institutes of Health, Bethesda, Maryland, USA,
641 https://imagej.nih.gov/ij/, 1997-2018.;
642 45. Talbot JC, Amacher SL. A streamlined CRISPR pipeline to reliably generate zebrafish
643 frameshifting alleles. Zebrafish. 2014 Dec;11(6):583–5.
644 46. Sutton BC, Allen RA, Zhao ZJ, Dunn ST. Detection of the JAK2V617F mutation by
645 asymmetric PCR and melt curve analysis. Cancer Biomarkers. 2007 Nov
646 16;3(6):315–24.
647
648

Figure Legends

Figure 1. *Staphylococcus aureus* location within neutrophils changes from vesicular to cytosolic throughout infection. (**A-B**) *Tg(mpx:eGFP)*i114 larvae were injected at 1 dpf with 1500 cfu SH1000 mCherry *S. aureus*, and imaged at early (1-5 hpi) and late (24-28 hpi) time points. (**A**) Number of bacteria contained in neutrophils, with maximum 100 bacterial cells counted (whole larvae imaged, n=11-13, Mann-Whitney test, ****p<0.0001, +/- SD). (**B**) Proportion of neutrophils containing bacteria (whole larvae imaged, n=11-12, unpaired t-test, ****p<0.0001, +/- SEM) (**C**) *Tg(mpx:eGFP)*i114 larvae were injected at 1 dpf with 1500 cfu SH1000 mCherry *S. aureus*, and imaged at 3 h post-infection. Images were captured every 5 min for 12 h at multiple z planes to follow infected neutrophils over time (scale: 5 µm). (**D-G**) *Tg(lyz:RFP-GFP-lc3)*sh383 larvae were injected at 2 dpf with GFP *S. aureus*, and imaged in the CHT at 2 hpi, and ~26 hpi. (**D**) The proportion of infected or non-infected neutrophils at 2 hpi and 26 hpi (****p<0.0001 Chi-Square test, n=3, 17 2 hpi larvae, 11 26 hpi larvae). (**E**) *S. aureus* with Lc3 marking the entire vesicle (scale: 9 µm), demonstrating a vesicle. (**F**) *S. aureus* in the cytosol (scale: 9 µm). (**G**) Proportion *S. aureus* events observed within vesicles or cytosol at 2 hpi and 26 hpi (***p<0.001, Fisher's exact test, n=3, 17 larvae at 2 hpi, and 11 larvae at 26 hpi).

Figure 2. *In vivo* recruitment of GFP-Sqstm1 puncta during *S. aureus* infection. (**A**) Representative image of *S. aureus* observed within a likely "vesicle" with GFP-Sqstm1 puncta localization, (scale: 7 µm) (**B**) representative image of *S. aureus* observed within the cytosol with GFP-Sqstm1 puncta localization, (scale: 9 µm) (**C**) *S. aureus* within vesicles, co-localized with GFP-Sqstm1 at 2 hpi and 26 hpi (CHT imaged, ns, Fisher's exact test, n=3, 14 larvae at 2 hpi, and 12 larvae at 26 hpi) (**D**) *S. aureus* in the cytosol, co-localized with GFP-Sqstm1 at 2 hpi and 26 hpi (CHT imaged, *p<0.05, Fisher's exact test, n=3, 14 larvae at 2 hpi, and 12 larvae at 26 hpi) (**E**) GFP-Sqstm1 puncta in the cytosol of infected and non-infected at 2 hpi (CHT imaged, ns, Mann-Whitney test, n=3, error bars +/- SD, 14 larvae) (**F**) GFP-Sqstm1 puncta in the cytosol of infected and non-infected at 26 hpi (CHT imaged, **p<0.01, Mann-Whitney test, n=3, error bars +/- SD, 12 larvae) (**G-I**) 2500 cfu of GFP *S. aureus* injected into *Tg(lyzC:RFP-GFP-lc3)sh383*, larvae imaged in the CHT at 2 hpi and 26 hpi. (**G**) Lc3 association to the entire *S. aureus* vesicle at 2 hpi and 26 hpi (ns, Fisher's test, n =3, 17 2 hpi larvae, 11 26 hpi larvae) (**H**) The number of *S. aureus* vesicles with Lc3 puncta (*p<0.05, Fisher's test, n =3, 17 2 hpi larvae, 11 26 hpi larvae) (**I**) The number of *S. aureus* events in the cytosol with Lc3 puncta at 2 hpi and 26 hpi (ns, Fisher's test, n =3, 17 larvae at 2 hpi, 11 larvae at 26 hpi).

Figure 3. Zebrafish survival is reduced following infection with *Staphylococcus aureus* in the absence of Sqstm1. (**A-B**) Zebrafish survival following *S. aureus* infection, larvae were injected with 1500 cfu of SH1000 at 30 hpf. (**A**) *sqstm1* morphants or control morphants survival (n=3, 74-80 larvae per group, p=0.004, Log-rank, Mantel-Cox test) (**B**) *sqstm1* mutant or wild-type sibling survival (n=3, 57-60 larvae per group, p=0.0168, Log-rank, Mantel-Cox test) (**C**) Electropherograms showing the sequence of wild type and sh558 mutant Sqstm1. Dashed vertical lines show the location of the 5-bp deletion. The position of the frameshift in the Sqstm1 protein is illustrated. Since this frameshift is located in the final coding exon, we predict translation of a truncated Sqstm1 protein lacking the UBD domain. (**D-E**) Number of infected neutrophils at 26 hpi following *S. aureus* infection, larvae were injected with 1500 cfu of SH1000 mCherry (D) or GFP (E), imaging completed in CHT at 30 hpf (**D**) *sqstm1* mutant or wild-type sibling (n=3, 19-36 larvae per group, p=0.0168, p=0.1039, Mann-Whitney test, error bars +/- SEM) (**E**) *sqstm1* morphants or control morphants in *Tg(mpx:eGFP)*i114 larvae (n=3, 32-34 larvae per group, p=0.115, Mann-Whitney test, error bars +/- SEM) (**F**) Number of neutrophils containing cytosolic *S. aureus* in *sqstm1* morphants or control morphants *Tg(mpx:eGFP)*i114 larvae (n=3, 32-34 larvae per group, **p<0.01, Mann-Whitney test, error bars +/- SEM)

Figure 1

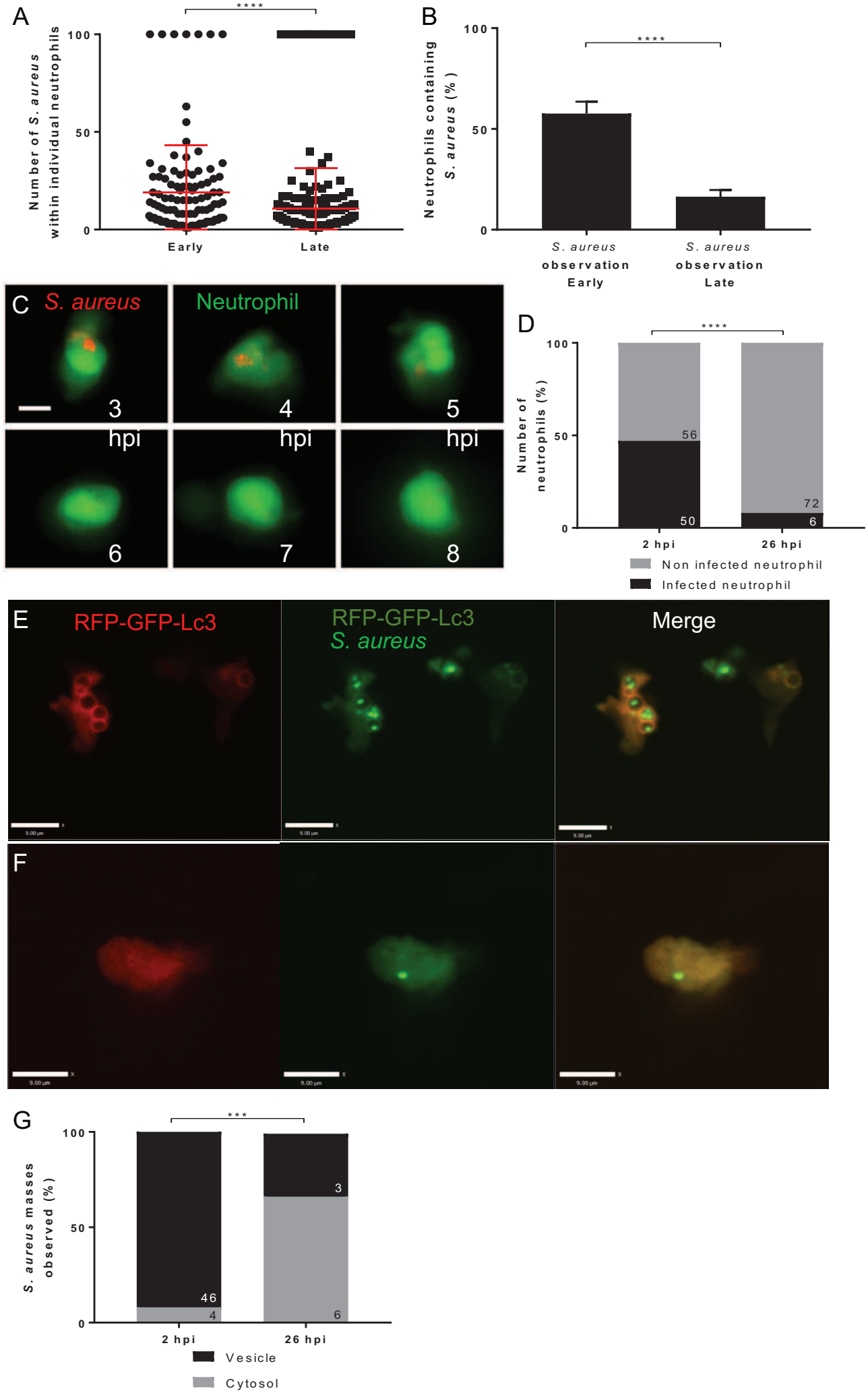
A
Number of S. aureus within individual neutrophils
100
50
0
****
Early
Late
B
Neutrophils containing S. aureus (%)
100
50
0
****
S. aureus observation Early
S. aureus observation Late
C
S. aureus
Neutrophil
3 hpi
4 hpi
5 hpi
6 hpi
7 hpi
8 hpi
D
Number of neutrophils (%)
100
50
0
****
56
50
72
6
2 hpi
26 hpi
Non infected neutrophil
Infected neutrophil
E
RFP-GFP-Lc3
RFP-GFP-Lc3
S. aureus
Merge
F
G
S. aureus masses observed (%)
100
50
0
***
46
4
3
6
2 hpi
26 hpi
Vesicle
Cytosol

Figure 2

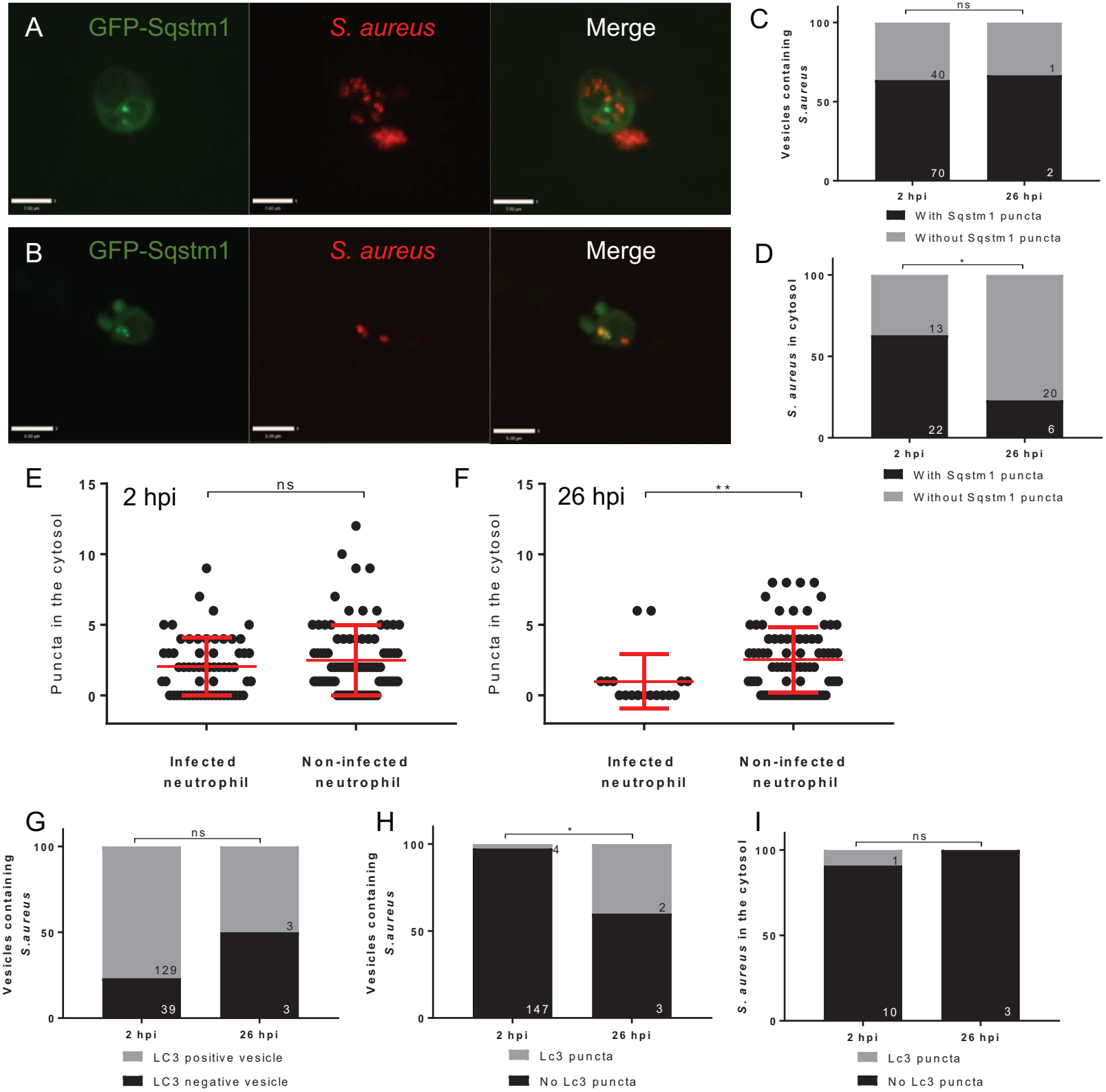
A
GFP-Sqstm1
S. aureus
Merge
B
GFP-Sqstm1
S. aureus
Merge
C
ns
Vesicles containing S.aureus
100
50
0
40
70
1
2
2 hpi
26 hpi
With Sqstm1 puncta
Without Sqstm1 puncta
D
*
S. aureus in cytosol
100
50
0
13
22
20
6
2 hpi
26 hpi
With Sqstm1 puncta
Without Sqstm1 puncta
E
2 hpi
ns
Puncta in the cytosol
15
10
5
0
Infected neutrophil
Non-infected neutrophil
F
26 hpi
**
Puncta in the cytosol
15
10
5
0
Infected neutrophil
Non-infected neutrophil
G
ns
Vesicles containing S.aureus
100
50
0
129
39
3
3
2 hpi
26 hpi
LC3 positive vesicle
LC3 negative vesicle
H
*
Vesicles containing S.aureus
100
50
0
4
147
2
3
2 hpi
26 hpi
Lc3 puncta
No Lc3 puncta
I
ns
S. aureus in the cytosol
100
50
0
1
10
3
2 hpi
26 hpi
Lc3 puncta
No Lc3 puncta

Figure 3

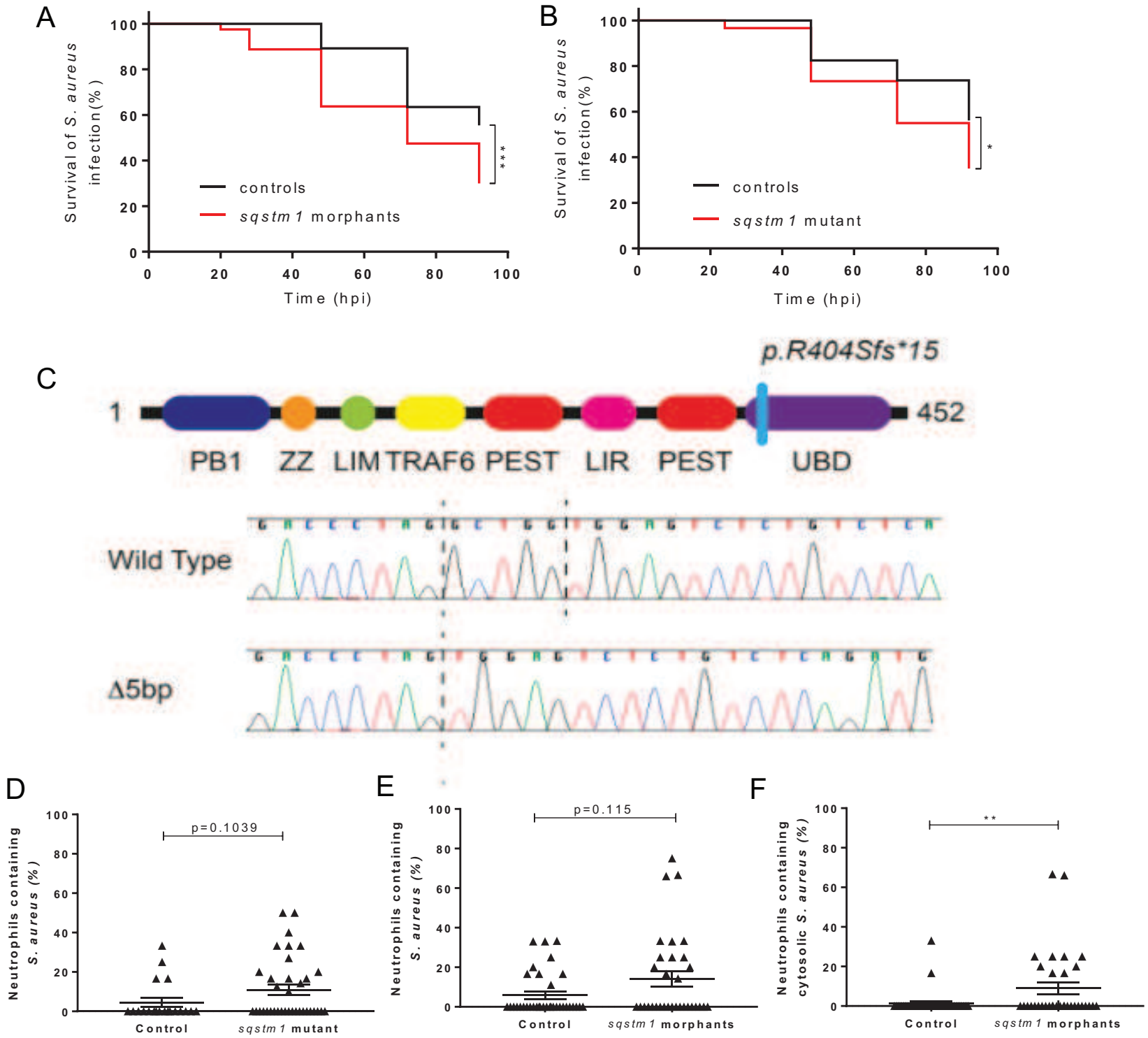
A
Survival of S. aureus infection(%)
Time (hpi)
controls
sqstm1 morphants
***
B
Survival of S. aureus infection(%)
Time (hpi)
controls
sqstm1 mutant
*
C
p.R404Sfs*15
1
452
PB1
ZZ
LIM
TRAF6
PEST
LIR
PEST
UBD
Wild Type
Δ5bp
D
Neutrophils containing S. aureus (%)
p=0.1039
Control
sqstm1 mutant
E
Neutrophils containing S. aureus (%)
p=0.115
Control
sqstm1 morphants
F
Neutrophils containing cytosolic S. aureus (%)
**
Control
sqstm1 morphants